

## Improved efficiency of MEH-PPV:PCBM solar cells by the use of ZnS nano-particles

Manju Shukla · Nameeta Brahme

Received: 19 December 2010 / Revised: 8 March 2011 / Accepted: 13 May 2011 /

Published online: 20 May 2011

© Springer-Verlag 2011

**Abstract** Zinc sulphide (ZnS) nano-particles ( $\sim 10$  nm) have been synthesized and incorporated in poly(2-methoxy-5-(2-ethylhexyloxy)-1,4-phenylenevinylene) (MEH-PPV) for photovoltaic applications. Incorporation of ZnS nano-particles in MEH-PPV improved the photovoltaic performance, as they work as electron acceptors and provide better electron transport in the matrix. ZnS nano-particles have also been dispersed in MEH-PPV along with phenyl [6,6'] C<sub>61</sub> butyric acid methyl ester (PCBM). Incorporation of optimum amount of ZnS nano-particles in MEH-PPV:PCBM system resulted into further increase in the power conversion efficiency compared to that in their absence. This improvement in the efficiency has been attributed to additional better pathways for electron transportation.

**Keywords** Zinc sulphide · Polymer solar cell · MEH-PPV · PCBM

### Introduction

In the present time, where demand of energy is increasing day by day and various alternate sources of energy are being developed, polymer solar cells are drawing more and more attention because of their prospects of being eco-friendly, flexible and cost effective [1, 2]. Since the early report on respectable power conversion efficiency in polymer solar cell, their performance has improved enormously [3–5]. Efforts are been made throughout the world to develop these devices via understanding the device physics, synthesis and application of new advanced materials and various treatments to the materials and devices [6–17], which have led these devices to high efficiencies. The best efficiency reported one decade earlier hardly reached beyond 1%, whereas efficiency more than 7% has been achieved

M. Shukla (✉) · N. Brahme

School of Studies in Physics, Pt. Ravishankar Shukla University, Raipur 492010, CG, India  
e-mail: manjushukla2003@gmail.com

today [3–5, 13]. However, the performance of these devices is not sufficient enough for their commercialization, and further efforts are necessarily required to improve further the performance and make them commercially viable.

There are various factors which limit the efficiency of polymer solar cells, where inefficient light absorption, high exciton binding energy, low exciton diffusion lengths, poor charge separation, transportation and collection are some of the examples. It is note worthy that most of the conjugated polymers used for electronic applications are amorphous in nature and possess low charge carrier mobilities. Because of low charge carrier mobilities, the charge carrier collection is not efficient and it results into low efficiencies in these devices. By the use of materials with high charge carrier mobilities, the efficiency of the devices is expected to increase further. Therefore, with the hope of better efficiencies, research is being done on hybrid solar cells, which incorporate nano-structured inorganic materials (ZnO, ZnS, CdSe, PbS, etc.) along with the conjugated polymers [18–22]. The hybrid organic–inorganic solar cells utilize the solution processibility of polymers and high electron mobility of inorganic counterparts for efficient collection of charge carriers at the electrodes. High surface to volume ratio of the nano-structured inorganic materials also extends the interfacial area with the polymers and makes sure the efficient dissociation of excitons. More detail on the hybrid organic–inorganic solar cells can be found in the reviews available in the literature [23, 24].

In view of the same objectives, we have synthesized and dispersed the ZnS nano-particles in MEH-PPV and investigated the photovoltaic performance. Devices prepared by the dispersion of ZnS nano-particles in MEH-PPV exhibited relatively poor photovoltaic performance compared to those prepared by the blend of MEH-PPV and PCBM. On the other hand, dispersion of ZnS nano-particles in MEH-PPV:PCBM system exhibited further improvement in the photovoltaic performance, which has been attributed to the improved electron transport by better pathways. MEH-PPV works as electron donor in both the systems, whereas ZnS and PCBM work as electron acceptors.

## Experimental details

Nano-particles of ZnS were synthesized via wet chemical route, where 0.01 M solutions of sodium sulphide ( $\text{Na}_2\text{S}$ ) (10 mL) in water was mixed dropwise in the 0.01 M solution of zinc acetate dihydrate ( $\text{Zn}(\text{CH}_3\text{COO})_2 \cdot 2\text{H}_2\text{O}$ ) (10 mL) in ethanol. All the chemicals used in the synthesis of ZnS nano-particles were purchased from Acros Organics. The reaction was carried out in an ultrasonic bath at room temperature. With addition of  $\text{Na}_2\text{S}$  solution in  $\text{Zn}(\text{CH}_3\text{COO})_2 \cdot 2\text{H}_2\text{O}$  solution, grayish colloidal particles of ZnS were precipitated, and the reaction medium was kept under continuous ultrasonication for ~1 h. The mixture was now centrifuged and sequentially washed with ethanol and water for five times. Subsequently, the precipitate was filtered out via vacuum and suction process using Millipore 0.1 micron filter assembly and then dried in the vacuum oven at 80 °C for 2 h to get the light grayish nano-particles of ZnS. The beauty of these particles is that no capping agent has been used here to control the size of the particles. The

reaction condition was self-controlling to get the nano-particles. It is important to note that the use of capping agents over the nano-particles inhibits the direct interaction of particles with the polymer when they are mixed with. Also the capping agents inhibit the electron transfer from polymer to nano-particles, which results poor photovoltaic performance. The particles synthesized here were characterized by X-ray diffraction (XRD) and high resolution transmission electron microscope (HRTEM) studies. From the HRTEM images, the average size of the particles was measured to be  $\sim 10$  nm. For HRTEM studies, the ZnS nano-particles (10 wt%) were dispersed by ultrasonication in 15 mg/mL solution of MEH-PPV in chlorobenzene, and then the solution was diluted 10 times by chlorobenzene. A drop of the diluted solution was poured onto the copper grid (used for TEM studies) to get a very thin film of the composite which was then dried at 80 °C for 30 min in the vacuum oven. Finally, these grids were used for HRTEM studies.

The devices were prepared on the indium tin oxide (ITO)-coated glass substrates in the configuration ITO/poly(ethylene-dioxythiophene):poly(styrene sulfonate) (PEDOT:PSS)/active layer/Al. Prior to device preparation, the ITO substrates ( $\sim 18 \Omega/\square$ ) were patterned in strip-like structure by photolithography technique with a width of 3 mm. After that the substrates were cleaned properly with soap solution, acetone, trichloroethylene and iso-propanol, and then dried in vacuum oven at 120 °C for 1 h. PEDOT:PSS (1.3 wt% dispersion in H<sub>2</sub>O, conductive grade with conductivity of 1 S/cm) was spun on the substrates at 2,000 rpm for 1 min and then cured at 100 °C for 30 min in the vacuum oven. The active layers were prepared via spin coating of the blend solutions of MEH-PPV with ZnS and/or PCBM at 2,000 rpm for 2 min and then curing at 120 °C for 30 min in a glove box. The glove box was filled with pure and dry nitrogen gas. MEH-PPV, PCBM, and PEDOT:PSS were purchased from Aldrich Chemicals and used as such. The solutions of MEH-PPV, PCBM, and ZnS were prepared separately in chlorobenzene with a concentration of 15 mg/mL and ultrasonicated for 30 min at 50 °C. Once the solutions were ready, they were mixed in appropriate ratio to get the desired recipes, and the mixtures were again ultrasonicated for 15 min at 50 °C. For preparation of solar cells, ZnS nano-particles were dispersed in MEH-PPV with 50 wt% ratio, whereas PCBM was mixed in MEH-PPV with 80% weight ratio. ZnS nano-particles were also mixed in MEH-PPV:PCBM (1:4) blend in different wt% ratio to investigate the photovoltaic response. Cathode in the present devices was an Al electrode and was deposited by thermal evaporation of Al (200 nm) through shadow masks (with 3 mm line openings) in a vacuum chamber at base pressure of  $\sim 1 \times 10^{-5}$  Torr. The Al electrodes were deposited in the cross geometry to the ITO strips to get the active area of 9 mm<sup>2</sup>. To avoid performance variation due to processing conditions, all the samples were prepared in identical conditions. After preparation, the devices were cured at 150 °C for 5 min in the glove box. UV-vis absorption spectrophotometer 2401PC from Shimadzu was used for absorption studies whereas a Keithley 2400 source measure unit, interfaced with computer was used to study the current density–voltage (*J*–*V*) characteristics of the devices. For the photovoltaic studies of the devices were illuminated at 1 sun (100 mW/cm<sup>2</sup>) using a Newport solar simulator with AM 1.5G irradiance.

## Results and discussion

Figure 1 shows the XRD graph of the nano-particles and indicates their crystalline nature. The peak positions represent the formation of cubic zinc blend crystalline structure of the particles with three crystallographic planes at (111), (220), and (311). Inset shows the HRTEM micrograph of ZnS nano-particles dispersed in MEH-PPV matrix. However, it is observed that the dispersion of particles is not completely uniform and forms aggregates at some places. The formation of slight aggregates are expected as the particles are not capped with the capping agent and do form phase separation. It can clearly be seen from the micrograph, the average size of the particles is  $\sim 10$  nm. The magnified image of a particle indicates the crystalline nature which was also confirmed by XRD. Figure 2 shows the UV-visible absorption spectra of MEH-PPV, PCBM, and ZnS nano-particles in their chlorobenzene solutions. MEH-PPV exhibits a strong absorption within the visible range from  $\sim 550$  to  $\sim 390$  nm with maximum absorption at  $\sim 500$  nm, whereas PCBM absorbs in the range  $\sim 575$  to  $\sim 300$  nm with the maximum absorption at  $\sim 343$  nm. ZnS nano-particles exhibited weak absorption in the visible range, whereas a rather strong absorption in ultraviolet range with a maximum at  $\sim 310$  nm. The absorption spectra of all the three materials MEH-PPV, PCBM, and ZnS nano-particles are complementary to each other and as a whole this combination covers most of the ultraviolet and visible range of the solar spectrum. It is important to mention that most part of the excitons is generated in MEH-PPV, whereas PCBM and ZnS do work as electron transport species. Figure 3 shows the photoluminescence (PL) spectra of MEH-PPV:ZnS thin films for different wt%

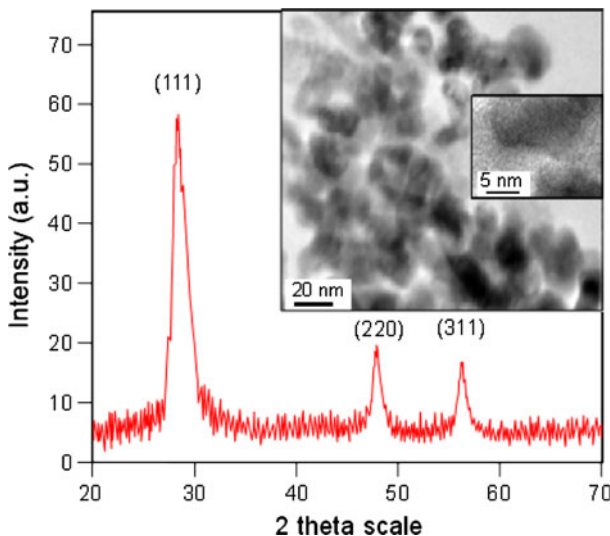


**Fig. 1** XRD graph of the ZnS nano-particles. The peaks positions correspond to the cubic zinc blend crystalline structure with three crystallographic planes at (111), (220), and (311). *Inset* shows the HRTEM image of the ZnS nano-particles dispersed in MEH-PPV matrix

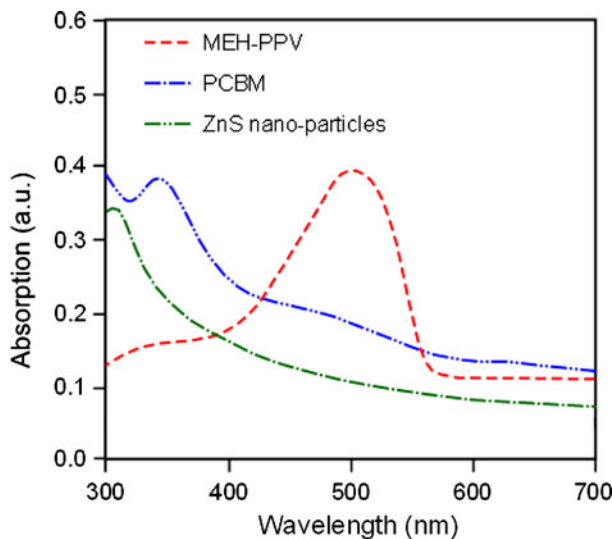


**Fig. 2** UV-visible absorption spectra of MEH-PPV, PCBM, and the synthesized ZnS nano-particles in chlorobenzene solution

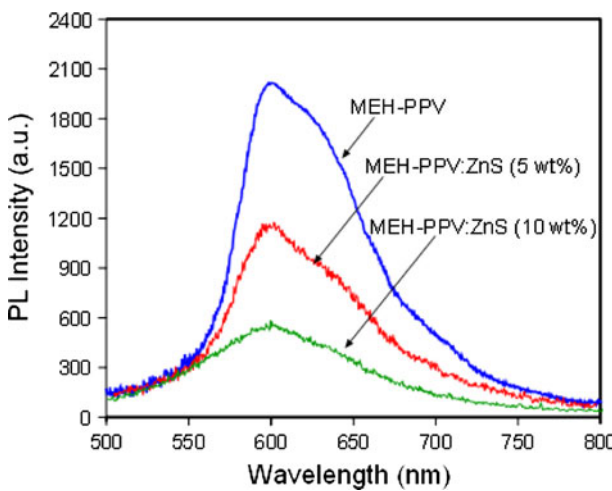


**Fig. 3** PL spectra of MEH-PPV:ZnS composite for different concentrations of ZnS nano-particles. Dispersion of ZnS nano-particle in MEH-PPV resulted into the PL quenching due to exciton dissociation and transfer of electrons from MEH-PPV to ZnS

concentrations of ZnS nano-particles. MEH-PPV exhibits PL spectrum ranging from ~550 to 750 nm with maximum at 600 nm. For PL studies, MEH-PPV was dissolved in chlorobenzene with the concentration of 1 mg/mL, and then ZnS nano-particles were dispersed in this solution. The PL spectra in Fig. 3 shows the relative variation of PL intensity with different wt% ratio of ZnS in MEH-PPV. Dispersion of ZnS nano-particles exhibited significant PL quenching in MEH-PPV which was

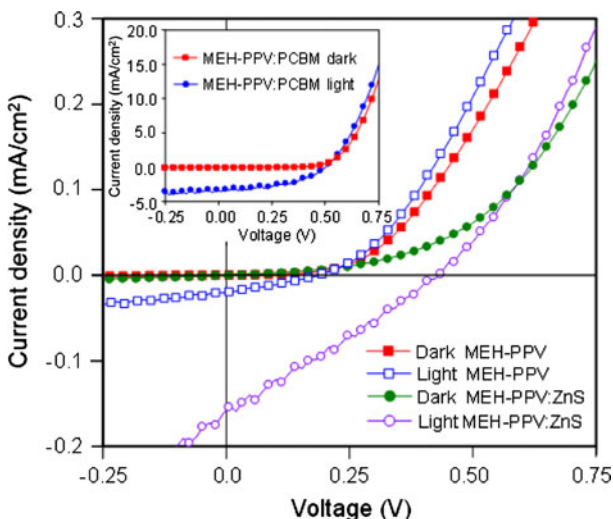
large for larger concentration of ZnS nano-particles. This PL quenching in the composite corresponds to the exciton dissociation and electron transfer from MEH-PPV to ZnS nano-particles. Thus, the ZnS nano-particles help in dissociation of excitons in the composite.

Figure 4 shows the  $J$ - $V$  characteristics of ITO/PEDOT:PSS/MEH-PPV/Al (*sample 1*) and ITO/PEDOT:PSS/MEH-PPV:ZnS (1:1)/Al (*sample 2*) devices measured in dark and under illumination at room temperature. Solid symbols are for the dark currents, whereas open symbols are for the currents measured under illumination. *Sample 1* exhibited very poor photovoltaic performance where short circuit current density ( $J_{sc}$ ), open circuit voltage ( $V_{oc}$ ), and fill factor (FF) were measured to be 0.02 mA/cm<sup>2</sup>, 0.18 V, and 0.30, respectively. The power conversion efficiencies ( $\eta$ ) of the devices have been calculated using the following relation:

$$\eta = \frac{J_{sc}V_{oc}\text{FF}}{P_{\text{in}}}, \quad (1)$$

where  $P_{\text{in}}$  is the optical power incident on the sample. The power conversion efficiency of *sample 1* was calculated to be 0.001%. However, *sample 2* exhibited relatively much better efficiency and was found to be 0.19%. *Sample 2* exhibited better  $J_{sc} = 1.6$  mA/cm<sup>2</sup> and  $V_{oc} = 0.42$  V, whereas the FF was found to be 0.28. This improvement in  $J_{sc}$  can be attributed to improved exciton dissociation and better electron transportation in the MEH-PPV:ZnS blend. The dispersion of ZnS nano-particles into MEH-PPV introduces the donor/acceptor interfaces which help in dissociation of excitons and provides better transport for collection of electrons at the cathode, which were rather difficult in pure MEH-PPV film. Compared to *sample 1*, *sample 2* exhibited more than two times  $V_{oc}$ .  $V_{oc}$  in organic photovoltaic devices can be attributed to the quasi-Fermi level splitting within the cell and is limited by the effective difference between highest occupied molecular orbital (HOMO) of donor and lowest unoccupied molecular orbital (LUMO) of the acceptor, minus some thermal limit (~300 meV) [25]. But it can be reduced by the poor contacts. The enhancement in  $V_{oc}$  in *sample 2* compared to that in *sample 1* can be attributed to the introduction of donor/acceptor interfaces where  $V_{oc}$  will be controlled by difference of HOMO of MEH-PPV and LUMO of ZnS nano-particles.

For comparison point of view, we prepared the solar cells using PCBM as an electron acceptor instead of ZnS nano-particles. It has been found that PCBM exhibits better photovoltaic performance when mixed with MEH-PPV in 80 wt% ratio [26, 27]. Therefore, devices were prepared using MEH-PPV and PCBM in 1:4 ratio. Inset of Fig. 4 shows the  $J$ - $V$  characteristics of MEH-PPV:PCBM solar cell measured in dark and under illumination at room temperature. The device with MEH-PPV:PCBM as the active layer exhibited much better performance with  $J_{sc} = 3.3$  mA/cm<sup>2</sup>,  $V_{oc} = 0.50$  V, FF = 0.49, and  $\eta = 0.80\%$ . The device with MEH-PPV:PCBM as an active layer exhibited an almost four times enhancement in the efficiency compared to that with MEH-PPV:ZnS nano-particles. This excellent improvement in the performance can be attributed to the phase separation and better nano-scale morphology of the MEH-PPV:PCBM active layer. It is worth mentioning that morphology of the active layer is a crucial parameter which controls the device performance. Shaheen et al. used poly(2-methoxy-5-(3'7'-dimethyloctyloxy)-1,4-phenylene-vinylene)



**Fig. 4** Dark and illuminated  $J$ - $V$  characteristics of ITO/PEDOT:PSS/MEH-PPV/Al (solid squares for dark and open squares for illumination) and ITO/PEDOT:PSS/MEH-PPV:ZnS (1:1)/Al (solid circles for dark and open circles for illumination) measured at room temperature. Inset shows the dark and illuminated  $J$ - $V$  characteristics of ITO/PEDOT:PSS/MEH-PPV:PCBM (1:4)/Al solar cell

(MDMO-PPV) as donor and PCBM as an acceptor and recorded a jump in efficiency from 0.9 to 2.5% by just using the appropriate solvent [12]. This improvement in the efficiency was because of better nano-scale morphology of the film. The solvents used for device fabrication were observed to have a crucial effect on the nano-scale morphology on the polymer films. Similarly Padinger et al. [6] fabricated polymer solar cells based on poly(3-hexylthiophene) (P3HT):PCBM and a post production thermal treatment to the device at 75 °C improved the efficiency from 0.4 to 2.5%. Along with this, the post production thermal treatment to the device at 75 °C in the presence of an externally applied voltage 2.7 V resulted into the overall efficiency of 3.5%. This improvement in the efficiency due to thermal annealing has been attributed to the improved nano-scale morphology, and better charge carrier transport in the active layer. Therefore, nano-scale morphology plays a very important role in polymer solar cells performance.

Figure 5a and b, respectively, shows the atomic force microscope (AFM) images of MEH-PPV:PCBM and MEH-PPV:ZnS nano particle thin films. It can be clearly seen from Fig. 5 that MEH-PPV:ZnS film possesses large roughness compared to MEH-PPV:PCBM film. Since the efficient solar cells demand excellent phase separation of donor and acceptor materials for better charge transportation, the relatively lower efficiency of MEH-PPV:ZnS device is because of poor phase separation of ZnS nano-particles that result relatively poor collection of charge carriers at the electrodes. Because of large roughness of MEH-PPV:ZnS film, the subsequent deposition of cathode on the film would not form a good contact and it would result poor photovoltaic performance [28, 29]. Since ZnS nano-particles are supposed to have better electron mobility therefore to utilize this benefit, we

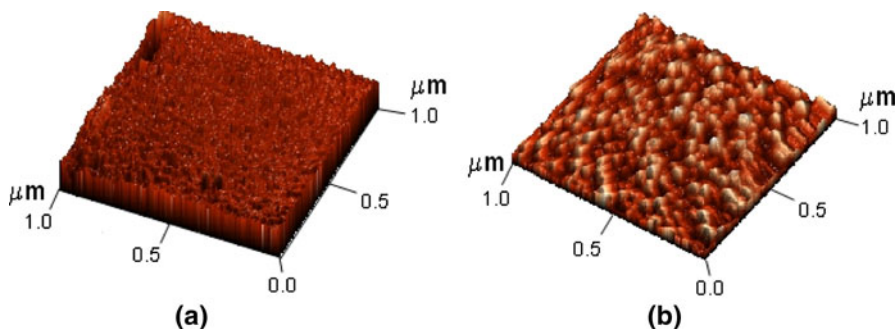


**Fig. 5** Atomic force microscope (AEM) images of thin films of **a** MEH-PPV:PCBM and **b** MEH-PPV:ZnS nano-particles prepared on glass/ITO/PEDOT:PSS substrates

**Table 1** Photovoltaic performance of ITO/PEDOT:PSS/MEH-PPV:PCBM (1:4):ZnS nano-particles ( $x$  wt%)/Al devices measured under  $100 \text{ mW/cm}^2$  illumination

	Active layer	$J_{sc}$ ( $\text{mA/cm}^2$ )	$V_{oc}$ (V)	FF (%)	$\eta$ (%)
Device A	MEH-PPV:PCBM (1:4):ZnS (0%)	3.3	0.50	49	0.80
Device B	MEH-PPV:PCBM (1:4):ZnS (5%)	3.9	0.50	52	1.01
Device C	MEH-PPV:PCBM (1:4):ZnS (10%)	5.7	0.51	44	1.29
Device D	MEH-PPV:PCBM (1:4):ZnS (20%)	4.1	0.51	34	0.71

Here  $x$  has been varied from 0 to 20 wt%

additionally incorporated ZnS nano-particles in MEH-PPV:PCBM (1:4) system and studied the photovoltaic performance.

For detailed analysis and optimization, the ZnS nano-particles were incorporated in different wt% ratio in MEH-PPV:PCBM. Incorporation of ZnS nano-particles in MEH-PPV:PCBM system has been observed to improve the performance first but for large concentration of ZnS nano-particles the performance deteriorated. The photovoltaic performance of solar cells based on the blend MEH-PPV:PCBM:ZnS nano-particles for different wt% ratio of ZnS nano-particles has been tabulated in Table 1, and the corresponding  $J$ - $V$  characteristics have been shown in Fig. 6. The optimum performance was observed for 10 wt% ratio of ZnS nano-particles in MEH-PPV:PCBM system, where the power conversion efficiency was observed to be 1.29%. The incorporation of ZnS nano-particles in MEH-PPV:PCBM system did not have any crucial effect on  $V_{oc}$  but increased the  $J_{sc}$ . This increment in  $J_{sc}$  is because of availability of better pathways for electron collection in MEH-PPV:PCBM:ZnS nano-particle system. As the conduction band of ZnS (3.7 eV) lies below the LUMO of MEH-PPV (3.1 eV) and PCBM (3.5 eV), incorporation of ZnS nano-particles in MEH-PPV:PCBM collects the electrons from both the MEH-PPV and PCBM, and additionally provide better mobility pathways for electrons. For larger concentration of ZnS nano-particles, the performance was observed to deteriorate and can be attributed to deterioration of nano-scale morphology of the active layer and formation of bad cathode interface.

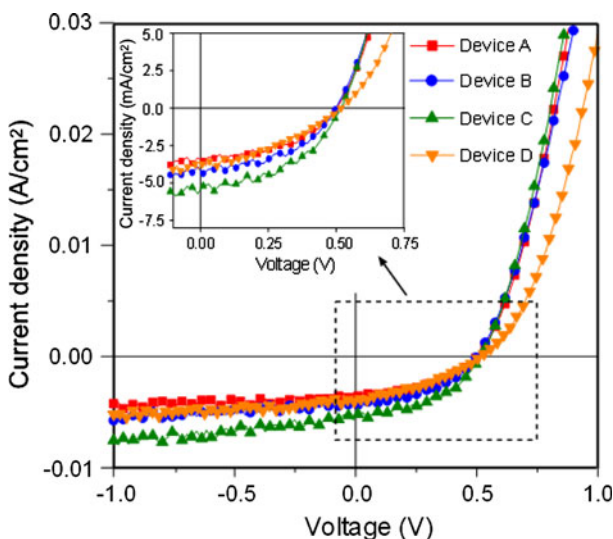


**Fig. 6** Illuminated  $J$ - $V$  characteristics of ITO/PEDOT:PSS/MEH-PPV:PCBM (1:4):ZnS ( $x$  wt%) / Al solar cells measured at room temperature. Here  $x$  has been varied from 0 to 20 wt%, and the devices have been designated as device A ( $x = 0$ ), device B ( $x = 5\%$ ), device C ( $x = 10\%$ ), and device D ( $x = 20\%$ ). *Inset* shows the magnified image of the marked region on the graph

## Conclusions

We have synthesized ZnS nano-particles ( $\sim 10$  nm) and incorporated with MEH-PPV to investigate the photovoltaic performance. Incorporation of ZnS nano-particles improved the photovoltaic performance as they work as electron acceptor in the system. However, the power conversion efficiency of MEH-PPV:ZnS nano-particle system was observed to be low, which has been attributed to poor phase separation, poor nano-scale morphology, and large surface roughness of the system. The optimum incorporation of ZnS nano-particles in MEH-PPV:PCBM system has been observed to improve further the power conversion efficiency and has been attributed to the additional better pathways for electron transportation. Though the performance of the devices reported in this article is not excellent, but it is expected to improve further by use of new advanced materials, processing devices in better experimental conditions, device optimization and different treatments. This article is an important contribution towards the use of inorganic ZnS nano-particles along with MEH-PPV:PCBM systems for better power conversion efficiencies.

**Acknowledgments** Authors would like to thank Indian Institute of Technology, Kanpur, National Physical Laboratory, New Delhi, and Indian Association for Cultivation Science, Kolkata, for providing the experimental facilities and material support for this work.

## References

1. Jain SC, Willander M, Kumar V (2007) Conducting organic materials and devices. Academic, San Diego, CA

2. Krebs FC, Spanggard H, Kjær T, Biancardo M, Alstrup J (2007) Mater Sci Eng B 138:106
3. Yu G, Heeger AJ (1995) J Appl Phys 78:4510
4. Yu G, Gao J, Hummelen J, Wudl F, Heeger AJ (1995) Science 270:1789
5. Liang Y, Xu Z, Xia J, Tsai ST, Wu Y, Li G, Ray C, Yu L (2010) Adv Mater 22:1
6. Padinger F, Rittberger RS, Sariciftci NS (2003) Adv Funct Mater 13:85
7. Peet J, Kim JY, Coates NE, Ma WL, Moses D, Heeger AJ, Bazan GC (2007) Nat Mater 6:497
8. Schilinsky P, Waldauf C, Hauch J, Brabec CJ (2004) J Appl Phys 95:2816
9. Waldauf C, Schilinsky P, Hauch J, Brabec CJ (2004) Thin Solid Films 451–452:503
10. Kumar P, Jain SC, Kumar V, Chand S, Tandon RP (2009) J Appl Phys 105:104507
11. Liang Y, Feng D, Wu Y, Sai ST, Li G, Ray C, Yu L (2009) J Am Chem Soc 131:7792
12. Shaheen SE, Brabec CJ, Sariciftci NS, Padinger F, Fromherz T, Hummelen JC (2001) Appl Phys Lett 78:841
13. Kim JY, Lee K, Coates NE, Moses D, Nguyen TQ, Dante M, Heeger AJ (2007) Science 317:222
14. Kumar P, Jain SC, Kumar H, Chand S, Kumar V (2009) Appl Phys Lett 94:183505
15. Cheng Y-J, Yang S-H, Hsu C-S (2009) Chem Rev 109:5868
16. Gunes S, Neugebauer H, Sariciftci NS (2007) Chem Rev 107:1324
17. Zhan X, Zhu D (2010) Polym Chem 1:409
18. Koster LJA, van Strien WJ, Beek WJE, Blom PWM (2007) Adv Funct Mater 17:1297
19. Beek WJE, Wienk MM, Janssen RAJ (2004) Adv Mater 16:1009
20. Gunes S, Fritz KP, Neugebauer H, Sariciftci NS, Kumar S, Scholes GD (2007) Sol Energy Mater Sol Cells 91:420
21. Landi BJ, Castro SL, Ruf HJ, Evans CM, Bailey SG, Raffaelle RP (2005) Sol Energy Mater Sol Cells 87:733
22. Bredol M, Matras K, Szatkowski A, Sanetra J, Schwab AP (2009) Sol Energy Mater Sol Cells 93:662
23. Boucle J, Ravirajan P, Nelson J (2007) J Mater Chem 17:3141
24. Helgesen M, Søndergaard R, Krebs FC (2010) J Mater Chem 20:36
25. Nelson J (2003) The physics of solar cells. Imperial College Press, London
26. Chang EC, Chao CI, Lee RH (2006) J Appl Polym Sci 101:1919
27. Jain SC, Aernout T, Kapoor AK, Kumar V, Geens W, Poortmans J, Mertens R (2005) Synth Met 148:245
28. Gupta D, Mukhopadhyay S, Narayan KS (2010) Sol Energy Mater Sol Cells 94:1309
29. Gupta D, Bag M, Narayan KS (2008) Appl Phys Lett 92:93301